



HAL
open science

Very high-order finite volume scheme for 1D convection diffusion problem: the implicit case

Gaspar Machado, Stéphane Clain, Rui M. S. Pereira

► To cite this version:

Gaspar Machado, Stéphane Clain, Rui M. S. Pereira. Very high-order finite volume scheme for 1D convection diffusion problem: the implicit case. 2012. hal-00675736

HAL Id: hal-00675736

<https://hal.science/hal-00675736>

Preprint submitted on 1 Mar 2012

HAL is a multi-disciplinary open access archive for the deposit and dissemination of scientific research documents, whether they are published or not. The documents may come from teaching and research institutions in France or abroad, or from public or private research centers.

L'archive ouverte pluridisciplinaire **HAL**, est destinée au dépôt et à la diffusion de documents scientifiques de niveau recherche, publiés ou non, émanant des établissements d'enseignement et de recherche français ou étrangers, des laboratoires publics ou privés.

Very high-order finite volume scheme for 1D convection diffusion problem: the implicit case

G. J. Machado^{a,*}, S. Clain^{a,b}, R. M. S. Pereira^a

^a Departamento de Matemática e Aplicações and CMAT, *Campus* de Azurém, 4800-058 Guimarães, Portugal

^b Institut de Mathématiques, CNRS UMR 5219, Université Paul Sabatier Toulouse 3, 118 route de Narbonne, F-31062 Toulouse cedex 4, France

*Corresponding author: gjm@math.uminho.pt

Abstract. *We present a fourth-order in space, second-order in time finite volume scheme for transient convection diffusion problem based on the Polynomial Reconstruction Operator and a Crank-Nicholson method. A detailed description of the scheme is provided and we perform numerical tests to highlight the performance of the method in comparison with the classical Patankar method.*

Keywords: Finite Volume; very high-order; transient convection-diffusion; Polynomial Reconstruction Operator (PRO).

1 Introduction

Efficient numerical schemes to solve convection diffusion equations is a constant challenge due to the wide range of problems which concern the coupling of the two major physical phenomena. Finite difference and finite element methods are very popular to produce numerical approximations ([1–3]) and a lot of academic and commercial codes are based on such techniques. The finite volume method for convection diffusion equations has been introduced in the sixties ([4, 5]) but did not receive attention during three decades whereas the finite element method has known a wide expansion. In the early eighties, the finite volume method reappeared with the original book of Patankar ([6]) for structured meshes and widely employed by engineers and physicists. Indeed, the method appears to be an interesting alternative due to its simplicity (one information per cell), the built-in conservative property, and the capacity to handle unstructured and non-conformal meshes. Important developments took place in this way and several classes of methods have been proposed. First, the original Patankar scheme for structured meshes has been extended to the non-structured case where an orthogonality condition is required to allow admissible diffusion flux (FV4 scheme [7–10]). The diamond scheme based on a local reconstruction of the gradient on each edge has been introduced by [11–13] while a finite volume scheme based on primal and dual meshes (DDFV scheme) has been proposed and developed by [14–16]. In the last six years, new techniques to design efficient finite volume schemes have been developed and a large proposal of numerical algorithms is now available such as the mixed-hybrid schemes ([17, 18]), mimetic schemes ([19, 20]), and schemes based on a local polynomial reconstruction ([21–23]).

Despite a constant effort to improve the schemes, a serious drawback of the finite volume method is the large amount of numerical viscosity and the weak convergence rate (at most second-order convergence). In the finite volume context, mean values are the fundamental data and the traditional (and implicit) identification "mean values = point-wise value at centroid" used by most of the authors is responsible of the discrepancy leading to, at most, a second-order scheme. The fact to reject such an identification is the crucial aspect of the presented method to provide fourth-order accuracy schemes. The main tool of the method is a local polynomial reconstruction in which the coefficients are determined from the mean values of the neighboring cells ([24, 25]). Another important issue is the choice of the reconstruction in function of the differential operator type. For the convective operator, we only employ internal values, *i.e.* mean-values on the cells, to determine the reconstructed polynomial function, whereas we introduce the Dirichlet conditions in the polynomial reconstruction employed in the diffusive operator to enforce

the boundary conditions.

This paper is devoted to a new class of finite volume schemes for transient convection-diffusion problem able to reach a fourth-order in space and second-order in time. We present the method for the one-dimensional case to detail the scheme with simple examples considering the convection-diffusion equation with the formulation

$$\begin{aligned} \partial_t u - \partial_x(a \partial_x u) + \partial_x(vu) &= f \quad \text{on } \Omega \times]0, T[\\ u(0, t) &= u_{\text{lf}}(t), \quad u(1, t) = u_{\text{rg}}(t), \quad u(x, 0) = u^0(x), \end{aligned}$$

where $\Omega :=]0, 1[$, a (the diffusive coefficient) and v (the convective coefficient) are regular functions on $\bar{\Omega} \times [0, T]$ with $a(x, t) \geq \alpha > 0$, while $f = f(x, t)$ represents a regular source term.

The rest of the paper is as follows. The second section recalls the classical finite volume scheme for convection-diffusion problem (namely the Patankar method). Then, we introduce several polynomial reconstructions in section three, while the fourth section is devoted to the high-order finite volume schemes. The next section concerns the numerical tests to show the scheme capacity to provide fourth-order in space and second-order in time accuracy both for the convective and the diffusive part of the operator. In the last section we present the conclusions and extensions.

2 Patankar finite volume schemes

To design the numerical schemes, we denote by \mathcal{T}_h a mesh of Ω constituted of cells $K_i := [x_{i-1/2}, x_{i+1/2}]$, $i = 1, \dots, I$, with centroid c_i , where $x_{1/2} := 0$ and $x_{i+1/2} := x_{i-1/2} + h_i$, and set h_r as the ratio between the length of two consecutive cells, that is $h_r := h_i/h_{i+1}$, $i = 1, 3, \dots, I-1$ (*cf.* Fig. 1). In the same way, we consider a

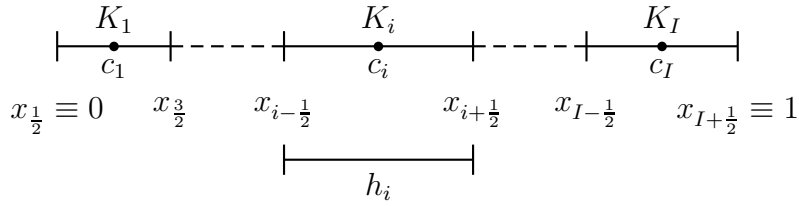


Figure 1: Mesh, cells and interface notations

subdivision $(t^n)_{n=0, \dots, N}$ of the time interval $[0, T]$ with $t^{n+1} := t^n + \delta^{n+1/2}$.

In the finite volume context, u_i denotes an approximation of the mean value over cell K_i , that is

$$u_i^n \approx \frac{1}{h_i} \int_{K_i} u(x, t_n) dx,$$

and vector $U^n = (u_1^n, \dots, u_I^n)^T \in \mathbb{R}^I$ is the vector of the unknowns at time t^n .

For the sake of consistency, we recall the Patankar scheme. For each interface $x_{i+1/2}$, $i = 0, \dots, I$, we define the diffusive and the convective fluxes for any vector $U \in \mathbb{R}^I$ by

$$\mathcal{F}_{\text{diff}, i+1/2}^{\mathcal{P}}(U) := a(x_{i+1/2}) \frac{2(u_{i+1} - u_i)}{(h_i + h_{i+1})} \quad (1)$$

and

$$\mathcal{F}_{\text{conv}, i+1/2}^{\mathcal{P}}(U) := [v(x_{i+1/2})]^+ u_i + [v(x_{i+1/2})]^- u_{i+1}, \quad (2)$$

respectively, where we have set $h_0 := 0$, $h_{I+1} := 0$, $u_0 = u_{\text{lf}}$, $u_{I+1} = u_{\text{rg}}$ and we used the notation $[\alpha]^+ := (\alpha + |\alpha|)/2$, $[\alpha]^- := (\alpha - |\alpha|)/2$. Note that we have skip the time index for the sake of simplicity. Then we defined the finite volume operator for cell K_i associated to the Patankar fluxes (1)-(2) by

$$\mathcal{G}_i^{\mathcal{P}}(U; u_{\text{lf}}, u_{\text{rg}}, f) := - \left[\mathcal{F}_{\text{diff}, i+1/2}^{\mathcal{P}}(U) - \mathcal{F}_{\text{diff}, i-1/2}^{\mathcal{P}}(U) \right] + \left[\mathcal{F}_{\text{conv}, i+1/2}^{\mathcal{P}}(U) - \mathcal{F}_{\text{conv}, i-1/2}^{\mathcal{P}}(U) \right] - h_i f_i, \quad (3)$$

where f_i is an approximation of the mean value of f over cell K_i , that is

$$f_i \approx \frac{1}{h_i} \int_{K_i} f \, dx.$$

Using expression (3), we define the semi-discrete problem: find $U(t) = (u_1(t), \dots, u_I(t))^T$ such that

$$\begin{aligned} \frac{dU}{dt} + \mathcal{G}^{\mathcal{P}}(U; u_{\text{lf}}, u_{\text{rg}}, f) &= (0, \dots, 0)^T \\ U(0) &= U^0, \quad u_0(t) = u_{\text{lf}}(t), \quad u_{I+1}(t) = u_{\text{rg}}(t), \end{aligned}$$

with

$$U^0 := (u_1^0, \dots, u_I^0)^T, \quad u_i^0 := \frac{1}{h_i} \int_{K_i} u^0 \, dx, \quad i = 1, \dots, I,$$

and

$$\mathcal{G}^{\mathcal{P}}(U; u_{\text{lf}}, u_{\text{rg}}, f) := (\mathcal{G}_1^{\mathcal{P}}(U; u_{\text{lf}}, u_{\text{rg}}, f), \dots, \mathcal{G}_I^{\mathcal{P}}(U; u_{\text{lf}}, u_{\text{rg}}, f))^T \in \mathbb{R}^I$$

being the finite volume operator for the mesh \mathcal{T}_h .

The three classical time discretizations are

- the explicit scheme:

$$\mathcal{H}^{\mathcal{P}}(U^{n+1}; U^n, u_{\text{lf}}, u_{\text{rg}}, f) := \frac{U^{n+1} - U^n}{\delta^{n+1/2}} + \mathcal{G}^{\mathcal{P}}(U^n; u_{\text{lf}}, u_{\text{rg}}, f);$$

- the implicit scheme:

$$\mathcal{H}^{\mathcal{P}}(U^{n+1}; U^n, u_{\text{lf}}, u_{\text{rg}}, f) := \frac{U^{n+1} - U^n}{\delta^{n+1/2}} + \mathcal{G}^{\mathcal{P}}(U^{n+1}; u_{\text{lf}}, u_{\text{rg}}, f);$$

- the Crank-Nicholson scheme:

$$\mathcal{H}^{\mathcal{P}}(U^{n+1}; U^n, u_{\text{lf}}, u_{\text{rg}}, f) := \frac{U^{n+1} - U^n}{\delta^{n+1/2}} + \frac{1}{2} \mathcal{G}^{\mathcal{P}}(U^n; u_{\text{lf}}, u_{\text{rg}}, f) + \frac{1}{2} \mathcal{G}^{\mathcal{P}}(U^{n+1}; u_{\text{lf}}, u_{\text{rg}}, f).$$

In each case, one has to determine the vector U^{n+1} solution of the affine problem

$$\mathcal{H}^{\mathcal{P}}(U; U^n, u_{\text{lf}}, u_{\text{rg}}, f) = 0, \quad U \in \mathbb{R}^I.$$

3 The polynomial reconstructions

The main tool to provide very high-order approximations is the construction of a specific polynomial approximation. In the sequel, we shall consider two kinds of reconstructions. For each cell K_i , $i = 1, \dots, I$, we denote by $\nu(i)$ the stencil associated to it such that $i \notin \nu(i)$, *i.e.* a set of neighboring cells, and by $u_i(x; \nu(i), d) \in \mathbb{P}_d$ the polynomial reconstruction on cell K_i of degree d based on the stencil $\nu(i)$.

In practice, we build the stencil $\nu(i)$ in function of the polynomial degree d we shall reconstruct picking up the nearest $d + 1$ cells to K_i . A difficulty arises when dealing with cells which share a point with the boundary. The two proposed reconstructions vary in the manner that the boundary conditions are considered.

3.1 Design of polynomial $\hat{u}_i(x; \nu(i), d)$

For each cell K_i , $i = 1, \dots, I$, we consider the polynomial expression (we skip the $\nu(i)$ reference for the sake of simplicity)

$$\hat{u}_i(x; d) := u_i + \sum_{\alpha=1}^d \hat{\mathcal{R}}_{\alpha}^i \left[(x - c_i)^{\alpha} - \frac{1}{h_i} \int_{K_i} (x - c_i)^{\alpha} \, dx \right],$$

where the coefficients $\hat{\mathcal{R}}_{\alpha}^i$, $\alpha = 1, \dots, d$, are the minimizers of the functional

$$\hat{E}(\hat{\mathcal{R}}_{\alpha}^i) := \sum_{j \in \nu(i)} \left[\frac{1}{h_j} \int_{K_j} \hat{u}_i(x; d) \, dx - u_j \right]^2, \quad i = 1, \dots, I.$$

To provide the numerical flux at the boundary for the convective flux, we use the extension $\hat{u}_0 := u_{\text{lf}}$ and $\hat{u}_{I+1} := u_{\text{rg}}$ and we denote by $\hat{\mathcal{P}}(U; d) = (\hat{u}_0(x; d), \dots, \hat{u}_{I+1}(x; d))^T$ the vectorial function on Ω associated to the \hat{u} polynomial reconstruction.

3.2 Design of polynomial $\tilde{u}_i(x; \nu(i), \mathbf{d})$

For all the cells K_i , $i = 1, \dots, I$, we use the same polynomial function of the previous subsection, that is,

$$\tilde{u}_i(x; \mathbf{d}) := u_i + \sum_{\alpha=1}^{\mathbf{d}} \tilde{\mathcal{R}}_{\alpha}^i \left[(x - c_i)^{\alpha} - \frac{1}{h_i} \int_{K_i} (x - c_i)^{\alpha} dx \right].$$

For $i = 2, \dots, I - 1$, we set $\tilde{\mathcal{R}}_{\alpha}^i := \hat{\mathcal{R}}_{\alpha}^i$. To provide the reconstructed polynomial function for $i = 1$, we slightly modify the functional introducing the boundary condition, that is,

$$\tilde{E}(\tilde{\mathcal{R}}_{\alpha}^1) := (\tilde{u}_1(0) - u_{\text{lf}})^2 + \sum_{j \in \nu(0)} \left[\frac{1}{h_j} \int_{K_j} \tilde{u}_1(x; \mathbf{d}) dx - u_j \right]^2,$$

where we set $\nu(0) := \nu(1) - \{\text{last cell of } \nu(1)\}$. In the same way, we compute the last polynomial by minimizing functional

$$\tilde{E}(\tilde{\mathcal{R}}_{\alpha}^I) := \sum_{j \in \nu(I+1)} \left[\frac{1}{h_j} \int_{K_j} \tilde{u}_I(x; \mathbf{d}) dx - u_j \right]^2 + (\tilde{u}_I(1) - u_{\text{rg}})^2,$$

where now we set $\nu(I+1) := \nu(I) - \{\text{first cell of } \nu(I)\}$. We also introduce the polynomials $\tilde{u}_0 := \tilde{u}_1$, $\tilde{u}_{I+1} := \tilde{u}_I$ and denote by $\tilde{\mathcal{P}}(U; \mathbf{d}) = (\tilde{u}_0(x; \mathbf{d}), \dots, \tilde{u}_{I+1}(x; \mathbf{d}))^T$ the vectorial function on Ω associated to the \tilde{u} polynomial reconstruction.

4 PRO finite volume schemes

4.1 Finite volume formulation

The design of the finite volume schemes is based on the Polynomial Reconstruction Operator (PRO-FV-scheme). We use the $\tilde{\mathcal{P}}(U; \mathbf{d})$ reconstruction to approximate the diffusion flux while the polynomial reconstruction $\hat{\mathcal{P}}(U; \mathbf{d})$ is considered to compute the convective contribution. At last, the diffusive and the convective fluxes write, with $i = 0, \dots, I$,

$$\mathcal{F}_{\text{diff}, i+\frac{1}{2}}^{\text{PRO}}(U; u_{\text{lf}}, u_{\text{rg}}, f, \mathbf{d}) := a(x_{i+\frac{1}{2}}) \frac{\tilde{u}'_i(x_{i+\frac{1}{2}}; \mathbf{d}) + \tilde{u}'_{i+1}(x_{i+\frac{1}{2}}; \mathbf{d})}{2}$$

and

$$\mathcal{F}_{\text{conv}, i+\frac{1}{2}}^{\text{PRO}}(U; u_{\text{lf}}, u_{\text{rg}}, f, \mathbf{d}) := [v(x_{i+\frac{1}{2}})]^+ \hat{u}_i(x_{i+\frac{1}{2}}; \mathbf{d}) + [v(x_{i+\frac{1}{2}})]^- \hat{u}_{i+1}(x_{i+\frac{1}{2}}; \mathbf{d}),$$

respectively.

Based on the polynomial reconstruction and the definition of the fluxes, we now introduce the affine operator $U \rightarrow \mathcal{G}^{\text{PRO}}(U; u_{\text{lf}}, u_{\text{rg}}, f, \mathbf{d})$, from \mathbb{R}^I into \mathbb{R}^I given component by component by:

$$\begin{aligned} \mathcal{G}_i^{\text{PRO}}(U; u_{\text{lf}}, u_{\text{rg}}, f, \mathbf{d}) := & - \left[\mathcal{F}_{\text{diff}, i+\frac{1}{2}}^{\text{PRO}}(U; u_{\text{lf}}, u_{\text{rg}}, f, \mathbf{d}) - \mathcal{F}_{\text{diff}, i-\frac{1}{2}}^{\text{PRO}}(U; u_{\text{lf}}, u_{\text{rg}}, f, \mathbf{d}) \right] \\ & + \left[\mathcal{F}_{\text{conv}, i+\frac{1}{2}}^{\text{PRO}}(U; u_{\text{lf}}, u_{\text{rg}}, f, \mathbf{d}) - \mathcal{F}_{\text{conv}, i-\frac{1}{2}}^{\text{PRO}}(U; u_{\text{lf}}, u_{\text{rg}}, f, \mathbf{d}) \right] - h_i f_i. \end{aligned}$$

4.2 The semi-discrete formulation

Once again we consider U as a function of time from $[0, T]$ into \mathbb{R}^I , that is, $U(t) = (u_1(t), \dots, u_I(t))^T$, and we naturally extend the two polynomial reconstruction operators $\hat{\mathcal{P}}(U(t); \mathbf{d})$ and $\tilde{\mathcal{P}}(U(t); \mathbf{d})$ as a time parameter reconstruction providing polynomial functions for any time t . We then define the finite volume semi-discretization of order \mathbf{d} by

$$\mathcal{H}^{\text{PRO}}(U; u_{\text{lf}}, u_{\text{rg}}, f, \mathbf{d}) := \frac{dU}{dt} + \mathcal{G}^{\text{PRO}}(U; u_{\text{lf}}, u_{\text{rg}}, f, \mathbf{d}).$$

The semi-discrete problem consists in solving the affine system of I differential equations with the initial condition $U(0) = (u_1^0, \dots, u_I^0)^T$.

4.3 Time discretization

As in the Patankar case, we introduce the three classical time discretizations, namely

- the explicit scheme:

$$\mathcal{H}^{\text{PRO}}(U^{n+1}; U^n, \delta^{n+1/2}, u_{\text{lf}}, u_{\text{rg}}, f, \mathbf{d}) := \frac{U^{n+1} - U^n}{\delta^{n+1/2}} + \mathcal{G}^{\text{PRO}}(U^n; u_{\text{lf}}, u_{\text{rg}}, f, \mathbf{d});$$

- the implicit scheme:

$$\mathcal{H}^{\text{PRO}}(U^{n+1}; U^n, \delta^{n+1/2}, u_{\text{lf}}, u_{\text{rg}}, f, \mathbf{d}) := \frac{U^{n+1} - U^n}{\delta^{n+1/2}} + \mathcal{G}^{\text{PRO}}(U^{n+1}; u_{\text{lf}}, u_{\text{rg}}, f, \mathbf{d});$$

- the Crank-Nicholson scheme:

$$\mathcal{H}^{\text{PRO}}(U^{n+1}; U^n, \delta^{n+1/2}, u_{\text{lf}}, u_{\text{rg}}, f, \mathbf{d}) := \frac{U^{n+1} - U^n}{\delta^{n+1/2}} + \frac{1}{2}\mathcal{G}^{\text{PRO}}(U^n; u_{\text{lf}}, u_{\text{rg}}, f, \mathbf{d}) + \frac{1}{2}\mathcal{G}^{\text{PRO}}(U^{n+1}; u_{\text{lf}}, u_{\text{rg}}, f, \mathbf{d}).$$

In each case, one has to determine the vector U^{n+1} solution of the affine problem

$$\mathcal{H}^{\text{PRO}}(U; U^n, \delta^{n+1/2}, u_{\text{lf}}, u_{\text{rg}}, f, \mathbf{d}) = (0, \dots, 0)^T, U \in \mathbb{R}^I.$$

5 Numerical tests

Numerical simulations have been carried out to check the convergence order of the methods and show its effectiveness. Two kinds of convergence has to be investigated: one with respect to space discretization and the other with respect to time discretization.

In the following subsections, the error between the solution and its approximation is provided with L^∞ norm since we deal with regular functions, namely

$$E_0 := \max_{i=1}^I |u_i^N - \bar{u}_i^N|,$$

where

$$\bar{U} := (\bar{u}_1^N, \dots, \bar{u}_I^N), \quad \bar{u}_i^N := \frac{1}{h_i} \int_{K_i} u(x, T) dx,$$

are the exact mean values of the solution of the continuous problem at time $t = T$. Note that E_0 does not depend on the polynomial reconstruction but just on the mean values.

For the sake of simplicity, we consider a uniform dscretization in space and time controlled by parameters h and Δt so we set $h := h_i = \frac{1}{I}$, $i = 1, \dots, I$, and $\delta^{n+1/2} := \Delta t$, $n = 0, \dots, N$.

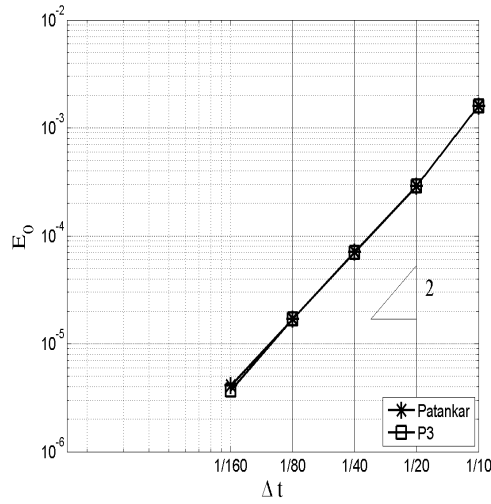
We will present two examples. In both of them, we have as the analytical solution $u(x, t) = \sin(2\pi x) \exp(-t)$. We take $a(x) = 1$ and $v = 0$ to provide a pure diffusion problem in the first example, while we consider a convection diffusion problem with $a(x) = 1$ and $v = 1$ in the second one. All the computations are performed using the Crank-Nicholson scheme in time till we reach the final time $T = 0.1$.

5.1 Example 1

As mentioned above, we first start with the transient diffusion equation. To measure the convergence rate deriving from the Crank-Nicholson method, we fix the number of cells large enough to guaranty a smaller error for the space approximation than the error deriving from the scheme in time. As expected, Table 1 shows that we get a second-order convergence both for the Patankar and the PRO- \mathbb{P}_3 (see the convergence curve in Figure 2). Note that we need 3200 cells to eliminate the error in space for Patankar while we only use 120 cell with the PRO-scheme. Another point is the better condition number of the linear system when using the PRO-scheme.

Table 1: Example 1 — convergence in time.

Δt	Patankar, $I = 3200$			\mathbb{P}_3 , $I = 120$		
	$k(A)$	E_0 err	ord	$k(A)$	E_0 err	ord
1/10	1.4E+06	1.6E−03	NA	1.7E+03	1.6E−03	NA
1/20	8.2E+05	2.9E−04	2.5	1.0E+03	2.9E−04	2.5
1/40	4.6E+05	7.1E−05	2.0	5.7E+02	7.0E−05	2.1
1/80	2.4E+05	1.7E−05	2.0	3.0E+02	1.7E−05	2.1
1/160	1.2E+05	4.1E−06	2.0	1.6E+02	3.7E−06	2.2

Figure 2: Example 1 — convergence curves of E_0 in time for a fixed value of I : $I = 3200$ for the Patankar scheme and $I = 120$ for the PRO-FV-scheme \mathbb{P}_3 (cf. Table 1).

We now check the convergence rate in space. To this end, we fix the time step small enough to ensure a neglected error in time. We obtain a predominant mass matrix leading to a small conditioning number but we need large number of iterations to reach the final time T . As shown in Table 2, we obtain a second-order scheme with the Patankar method, whereas an accurate and effective fourth-order is achieved with the PRO- \mathbb{P}_3 scheme. For 160 cells the error is cut by around 1000 with a smaller computational effort (see Figure 3 for the convergence curves).

Table 2: Example 1 — convergence in space with fixed $\Delta t = 1/1600$.

	I	$k(A)$	E_0	
			err	ord
Patankar	20	1.5E+00	7.4E−03	NA
	40	3.0E+00	1.9E−03	2.0
	80	9.0E+00	4.7E−04	2.0
	160	3.3E+01	1.2E−04	2.0
\mathbb{P}_3	20	1.4E+00	1.8E−03	NA
	40	2.7E+00	7.2E−05	4.7
	80	8.0E+00	3.7E−06	4.3
	160	2.9E+01	1.7E−07	4.4

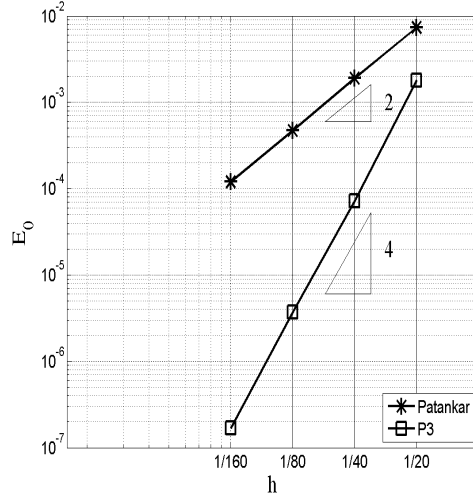


Figure 3: Example 1 — convergence curves of E_0 in space for a fixed value of $\Delta t (= 1/1600)$ (cf. Table 2).

Since the schemes in time and space have not the same order, it is numerically important to adapt the time step with the space step. For the Patankar scheme with Crank-Nicholson method, we have both a second-order scheme so we set $\Delta t = h$. Since the PRO- \mathbb{P}_3 provides a fourth-order in space, we set $\Delta t = h^2$ and expect a fourth-order convergence. Table 3 confirms the good choice of the time step and we get a global second-order scheme with Patankar and a global fourth-order scheme with the PRO method.

Table 3: Example 1 — convergence in space.

	I	$k(A)$	E_0 err	ord
Patankar ($\Delta t = h$)	10	1.4E+01	4.0E-02	NA
	20	3.3E+01	7.3E-03	2.5
	40	7.2E+01	1.8E-03	2.0
	80	1.5E+02	4.5E-04	2.0
	160	3.1E+02	1.1E-04	2.0
\mathbb{P}_3 ($\Delta t = h^2$)	10	2.6E+00	3.9E-02	NA
	20	2.7E+00	1.8E-03	4.4
	40	2.7E+00	7.2E-05	4.7
	80	2.7E+00	3.7E-06	4.3
	160	2.7E+00	2.1E-07	4.1

5.2 Example 2

The second example deals with the transient convection diffusion problem with $a(x) = 1$ and $v = 1$, and we choose the right-hand side term such that $u(x) = \sin(2\pi x) \exp(-t)$ is the solution. Based on the previous numerical experiences, we use $\Delta t = h$ for the Patankar-Crank-Nicholson scheme and $\Delta t = h^2$ for the PRO-Crank-Nicholson scheme. We print out in Table 4 the global convergence rate and obtain a first-order rate of convergence for the classical method due to the rough discretization of the convective part (just an upwind method). We obtain an effective fourth-order convergence with the PRO scheme which highlights the effectiveness of the method.

Table 4: Example 2 ($u(x) = \sin(2\pi x) \exp(-t)$, $a(x) = 1$, $v = 1$) with Crank-Nicholson

	I	$k(A)$	E_0 err	ord
Patankar ($\Delta t = h$)	10	1.4E+01	2.1E-02	NA
	20	3.3E+01	1.5E-02	0.5
	40	7.3E+01	9.9E-03	0.6
	80	1.5E+02	5.5E-03	0.9
	160	3.1E+02	2.9E-03	0.9
\mathbb{P}_3 ($\Delta t = h^2$)	10	2.7E+00	3.3E-02	NA
	20	2.8E+00	1.7E-03	4.2
	40	2.8E+00	7.2E-05	4.6
	80	2.8E+00	4.0E-06	4.2
	160	2.8E+00	2.3E-07	4.1

6 Conclusion

We have presented a new finite volume method for one-dimensional convection-diffusion problem which provides very high-order accuracy. Numerical simulations have been carried out to prove the capacity of the method to effectively reach the fourth-order accuracy. Several extensions are under consideration. The two- and three-dimensional case is of course of crucial importance, but we will also investigate the schemes for both Dirichlet and Neumann boundary conditions. Another difficulty concerns the solution stability when dealing with rough data. A strategy based on the MOOD method ([24, 25]) is currently being developed.

Acknowledgements: This research was financed by FEDER Funds through Programa Operacional Factores de Competitividade — COMPETE and by Portuguese Funds through FCT — Fundação para a Ciência e a Tecnologia, within the Project PEst-C/MAT/UI0013/2011.

7 Bibliography

REFERENCES

- [1] Z. Chen, Finite element methods and their applications, Springer-Verlag, (2005).
- [2] C. Grossmann, H.-G. Roos, and M. Stynes, Numerical treatment of partial differential equations, Springer-Verlag, (2007).
- [3] A. Tveito and R. Winther, Introduction to partial differential equations: a computational approach, Springer-Verlag, (1998).
- [4] A. A. Samarskii, On monotone difference schemes for the elliptic and parabolic equations in the case of a non-self-adjoint elliptic operator, Zh. Vychisl. Mat. i Mat. Fiz. 5 (1965), pp. 548–551 (in Russian).
- [5] A. N. Tichonov and A. A. Samarskii, Homogeneous difference schemes on nonuniform nets, Zh. Vychisl. Mat. i Mat. Fiz. 2 (1962), pp. 812–832 (in Russian).
- [6] S. V. Patankar, Numerical Heat Transfer and Fluid Flow, Series in Computational Methods in Mechanics and Thermal Sciences, McGraw Hill, (1980).
- [7] Z. Cai, On the finite volume element method, Numer. Math. 58 (1991), pp. 713–735.
- [8] Z. Cai, J. Mandel, and S. Mc Cormick, The finite volume element method for diffusion equations on general triangulations, SIAM J. Numer. Anal. 28 (2) (1991), pp. 392–402.
- [9] R. Eymard, T. Gallouët, and R. Herbin, Finite volume approximation of elliptic problems and convergence of an approximate gradient, Applied Numerical Mathematics 37 (2001), pp. 31–53.

-
- [10] R. Eymard, T. Gallouët, and R. Herbin, The finite volume method, Handbook for Numerical Analysis, Ph. Ciarlet J.L. Lions eds., North Holland, (2000), pp. 715–1022.
- [11] Y. Coudière, J.P. Vila, and P. Villedieu, Convergence rate of a finite volume scheme for a two dimensional convection diffusion problem, *Modél. Math. Anal. Numér.* 33 (3) (1999), pp. 493–516.
- [12] Y. Coudière and P. Villedieu, Convergence rate of a finite volume scheme for the linear convection-diffusion equation on locally refined meshes, *M2AN Math. Model. Numer. Anal.* 34 (6) (1999), pp. 1123–1149.
- [13] G. Manzini and A. Russo, A finite volume method for advection-diffusion problems in convection-dominated regimes, *Comput. Methods Appl. Mech. Engrg.* 197 (2008), pp. 1242–1261.
- [14] F. Hermeline, A finite volume method for the approximation of diffusion operators on distorted meshes, *J. Comput. Phys.* 160 (2000), pp. 481–499.
- [15] K. Domelevo and P. Omnes, A finite volume method for the Laplace equation on almost arbitrary two-dimensional grids, *M2AN Math. Model. Numer. Anal.* 39 (2005), pp. 1203–1249.
- [16] Y. Coudière and G. Manzini, The discrete duality finite volume method for convection-diffusion problems, *SIAM J. Numer. Anal.* 47 (6) (2010), pp. 4163–4192.
- [17] J. Droniou and R. Eymard, A mixed finite volume scheme for anisotropic diffusion problems on any grid, *Numer. Math.* 105 (2006), pp. 35–71.
- [18] R. Eymard, T. Gallouët, and R. Herbin, Benchmark on Anisotropic Problems. SUSHI: a scheme using stabilization and hybrid interfaces for anisotropic heterogeneous diffusion problems, *FVCA5 — Finite Volumes for Complex Applications V*, Wiley, (2008), pp. 801–814.
- [19] F. Brezzi, K. Lipnikov, and M. Shashkov, Convergence of Mimetic Finite Difference Methods for Diffusion Problems on Polyhedral Meshes, *SIAM J. Num. Anal.* 43 (2005), pp. 1872–1896.
- [20] A. Cangiani and G. Manzini, Flux reconstruction and solution post-processing in mimetic finite difference methods, *Computer Methods in Applied Mechanics and Engineering* 197 (9-12) (2008), pp. 933–945.
- [21] J.A. Hernández, High-order finite volume schemes for the advection-diffusion equation, *International Journal for Numerical Methods in Engineering*, 53 (2002), pp. 1211–1234.
- [22] C. Ollivier-Gooch and M. Van Altena, A high-order-accurate unstructured mesh finite-volume scheme for the advection-diffusion equation, *Journal of Computational Physics Archive* 181 (2) (2002), pp. 729–752.
- [23] E. F. Toro and A. Hidalgo, ADER finite volume schemes for nonlinear reaction-diffusion equations *Applied Numerical Mathematics archive* 59 (1) (2009), pp. 1–31.
- [24] S. Clain, S. Diot, and R. Loubère, A high-order polynomial finite volume method for hyperbolic system of conservation laws with Multi-dimensional Optimal Order Detection (MOOD), *Journal of Computational Physics* 230 (2011), pp. 4028–4050.
- [25] S. Clain, S. Diot, and R. Loubère, Multi-dimensional Optimal Order Detection (MOOD) — A very high-order Finite Volume Scheme for conservation laws on unstructured meshes, *FVCA6 — Finite Volumes for Complex Applications VI*, Springer Verlag, 1 (2011), pp. 263–271.